Do high-spin high mass X-ray binaries contribute to the population of merging binary black holes?

MONICA GALLEGOS-GARCIA,[1,2] MAYA FISHBACH,[2] VICKY KALOGERA,[1,2] CHRISTOPHER P L BERRY,[3,2] AND
ZOHEYR DOCTOR[2]

[1]*Department of Physics and Astronomy, Northwestern University, 2145 Sheridan Road, Evanston, IL 60208, USA*

[2]*Center for Interdisciplinary Exploration and Research in Astrophysics (CIERA),1800 Sherman, Evanston, IL 60201, USA*

[3]*SUPA, School of Physics and Astronomy, University of Glasgow, Glasgow G12 8QQ, UK*

ABSTRACT

Gravitational-wave observations of binary black hole (BBH) systems point to black hole spin magnitudes being relatively low. These measurements appear in tension with high spin measurements for high-mass X-ray binaries (HMXBs). We use grids of `MESA` simulations combined with the rapid population-synthesis code `COSMIC` to examine the origin of these two binary populations. It has been suggested that Case-A mass transfer while both stars are on the main sequence can form high-spin BHs in HMXBs. Assuming this formation channel, we show that depending on critical mass ratios for the stability of mass transfer, 48–100% of these Case-A HMXBs merge during the common-envelope phase and up to 42% result in binaries too wide to merge within a Hubble time. Both `MESA` and `COSMIC` show that high-spin HMXBs formed through Case-A mass transfer can only form merging BBHs within a small parameter space where mass transfer can lead to enough orbital shrinkage to merge within a Hubble time. We find that only up to 11% of these Case-A HMXBs result in BBH mergers, and at most 20% of BBH mergers came from Case-A HMXBs. Therefore, it is not surprising that these two spin distributions are observed to be different.

Keywords: Gravitational wave sources (677); Stellar mass black holes (1611); Stellar evolutionary models (2046); Roche lobe overflow (2155)

1. INTRODUCTION

Correct interpretation of gravitational-wave (GW) data and a complete understanding of black hole (BH) spin predictions from stellar and binary evolution are crucial to reveal the formation channels of merging binary BHs (BBHs). Of the BBH mergers detected by the LIGO Scientific, Virgo, and KAGRA Collaboration, most appear to have a small effective inspiral spin, $\chi_{\rm eff} \lesssim 0.2$–$0.3$ (Abbott et al. 2021b,a). The effective inspiral spin is a mass-weighted combination of the spin components aligned with the orbital angular momentum (Santamaría et al. 2010; Ajith et al. 2011), and hence it can be difficult to disentangle the component BH spin magnitudes from the spin–orbit alignment. Nevertheless, combining all the BBH mergers observed so far and fitting for the spin magnitude and tilt distributions, Abbott et al. (2021c) found that component spin magnitudes tend to be smaller than $\chi_i \sim 0.4$, a feature that could have implications for the understanding BH natal spins. Other important but contended features of the BBH spin distribution include the possibility of a zero-spin excess (Roulet et al. 2021; Galaudage et al. 2021), and the presence of systems with spin–orbit misalign-

ments larger than 90° (implying $\chi_{\rm eff} < 0$) (Abbott et al. 2021c,d). Implementing a series of hierarchical analyses of the BBH population, Callister et al. (2022) found preference for significant spin–orbit misalignment among the merging BBH population, but show that there is no evidence that GW data includes an excess of zero-spin systems. This latter point is in agreement with other studies (Kimball et al. 2020, 2021; Mould et al. 2022), and indicates that the majority of merging BBHs have small but non-zero spin (Abbott et al. 2021c).

The natal spins of BHs are largely determined by angular momentum (AM) transport from the core of the progenitor star to its envelope. If this AM transport is assumed to be efficient, it acts to decrease the rotation rate of the core as the envelope expands and loses AM through winds, resulting in BHs born from single stars with spins of $\sim 10^{-2}$ (Spruit 1999; Fuller et al. 2015; Fuller & Ma 2019). Evidence for efficient AM transport comes, in part, from comparison to observations of neutron star and white dwarfs spins (Heger et al. 2005; Suijs et al. 2008). However, we currently lack unambiguous evidence that AM transport is efficient in more massive stars, especially since there is no observed excess of zero-

spin systems in GW data. Additionally, Cantiello et al. (2014) found that this mechanism fails to reproduce the slow rotation rates of the cores of low-mass stars, which led to a revision of the AM transport process (Fuller et al. 2019). To further complicate this story, failed SN explosions can alter the spin of a new-born BH (Batta et al. 2017; Schrøder et al. 2018; Batta & Ramirez-Ruiz 2019), and binary evolution after the first BH is formed, like tidal synchronization, can increase the spin of the second-born BH, provided that the orbit is tight enough (Qin et al. 2018; Bavera et al. 2020; Fuller & Lu 2022).

High-mass X-ray binaries (HMXBs) consist of a compact object, either a neutron star or BH, with a massive donor star greater than $\gtrsim 5 M_\odot$ (Remillard & McClintock 2006; van den Heuvel 2019). Our focus is on high-mass X-ray binaries with BH accretors, and we refer to these as HMXBs for the rest of this paper. Of the three HMXBs with confident BH spin measurements (M33 X-7, Cygnus X-1 and LMC X-1), all BHs are observed to be highly spinning, with spin magnitudes $\gtrsim 0.8$ (Liu et al. 2008; Miller-Jones et al. 2021; Reynolds 2021). Although there are only three of these systems, it is clear that they have a distinct spin distribution compared to merging BBHs (Roulet & Zaldarriaga 2019; Reynolds 2021; Fishbach & Kalogera 2022).

We could naively expect that for both HMXBs and merging BBH systems, the spin of the first-born BH represents its natal spin. As discussed above, BH spins can be altered during a SN event or by strong binary interactions such as tides, which are likely to be more important for the second-born BH. While BBHs can be expected go through a HMXB phase, not all HMXBs will evolve to form merging BBHs (e.g. Belczynski et al. 2011, 2012; Miller-Jones et al. 2021; Neijssel et al. 2021). One goal of this paper to find an evolutionary path that can explain current observations: one that can impart large spin on the first-born BH in HMXBs but not in merging BBHs.

We must consider the possibility that these two classes of binaries may only appear different due to the limitations of how they are observed. Fishbach & Kalogera (2022) investigated whether the differences in the mass and spin distributions of HMXBs and merging BBHs may be a result of GW observational selection effects alone. Based upon GWTC-2 observations (Abbott et al. 2021e), they found that, accounting for GW observational selection effects and the small-number statistics of the observed HMXBs, the masses of the observed HMXBs are consistent with the BBH mass distribution. However, considering BH spins, the merging population of BBHs may include only a small subpopulation of systems that are HMXB-like (systems containing a rapidly

spinning component with $\chi \gtrsim 0.8$, and preferentially aligned with the orbital angular momentum axis, as expected from isolated binary evolution). Conservatively, Fishbach & Kalogera (2022) find that a HMXB-like population can make up at most 30% of merging BBH systems. It is therefore important to understand how the specific evolutionary pathways of merging BBHs and HMXBs shape their observed spins distributions (Liotine et al. 2022, in prep.).

We investigate if high-spin HMXBs are expected to contribute to the population of merging BBHs by modeling the evolution of these binaries. For the rest of this paper we will refer to the population of BBH systems that merge within a Hubble time as BBH. To identify high-spin HMXBs in our simulations, we assume the spin of the first-born BH is imparted by the scenario of Case-A mass transfer (MT) while both stars are on the main sequence (MS; Valsecchi et al. 2010; Qin et al. 2019). In this scenario, the donor star, which is also the progenitor of the first-born BH, could form a high-spin BH following a combination of (i) MT that prevents significant radial expansion; (ii) strong tidal synchronization at low orbital periods, and (iii) inefficient AM transport within the massive star post MS. We do not follow the spin evolution of these BH progenitors through this channel, but simply assume that systems following this Case-A MT formation path can form a maximally spinning first-born BH (Qin et al. 2019). We refer to these high-spin HMXBs as Case-A HMXBs. We show that only a small minority of Case-A HMXBs result in BBHs. Similarly, only a small fraction of BBHs had a Case-A HMXB progenitor. This implies that the BHs observed in HMXBs and those in BBHs predominantly belong to different astrophysical populations.

This paper is organized as follows. In Section 2 we outline our procedure for combining MESA and COSMIC simulations and provide an overview of the stellar and binary physics parameters used. In Section 3 we quantify how many Case-A HMXBs form BBHs, and what fraction of our total BBHs in the population had Case-A HMXB progenitors. In Section 4 we discuss caveats and avenues for future work. Finally, we summarize our findings in Section 5.

2. METHOD

We combine detailed binary evolution simulations modeled using MESA (Paxton et al. 2011, 2013, 2015, 2019) with simulations using the rapid population-synthesis code COSMIC (Breivik et al. 2020), which is based upon the evolutionary models of BSE (Hurley et al. 2002), to determine if Case-A HMXBs and BBHs originate from distinct populations. This combination al-

lows us to simulate large populations of binaries, and assess whether our results are robust by comparing them to populations informed by detailed simulations. Our simulations are computed using version 12115 of MESA, and version 3.4 of COSMIC. Our procedure for combing COSMIC and MESA simulations is similar to Gallegos-Garcia et al. (2021). Here we provide a brief summary and highlight any minor differences.
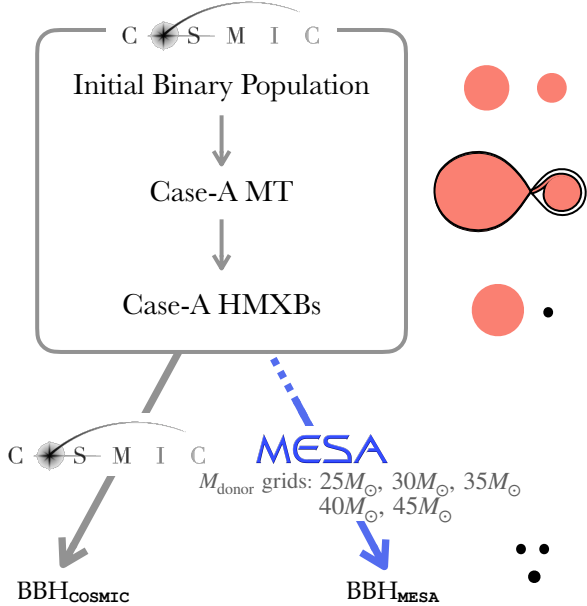

Figure 1. Illustration of method. The evolution of all binaries, from an initial ZAMS population, through Case-A MT while both stars are on the MS, to the formation of Case-A HMXBs, is simulated entirely with COSMIC. Starting from this population of Case-A HMXBs, we match each Case-A HMXBs to the nearest binary simulation in terms of orbital period and mass ratio from our grids of MESA simulations. For comparison, we use both COSMIC to simulate the remaining evolution.

We generate an initial population of binaries with COSMIC with multidimensional initial binary parameters following Moe & Di Stefano (2017). We evolve these binaries from zero-age MS (ZAMS) until the formation of a hydrogen-rich donor with a BH companion (BH–H-rich star). We refer to this as the HMXB stage. In this population, we highlight the systems that undergo Case-A MT while both stars are on the MS because these may result in high-spin HMXBs (Valsecchi et al. 2010; Qin et al. 2019). We refer to these systems as Case-A HMXBs. To compare our results across different donor masses at the BH–H-rich star stage, we separate these binaries into subpopulations determined by the donor mass. We consider five mass ranges in our COSMIC simulations, $M_{\mathrm{donor}} = (25 \pm 2.5)M_\odot$, $(30 \pm 2.5)M_\odot$,

$(35\pm2.5)M_\odot$, $(40\pm2.5)M_\odot$, and $(45\pm2.5)M_\odot$. We use a grid of MESA simulations at a *single* donor mass to compare to a selected mass range of COSMIC systems: i.e., a mass range of $M_{\mathrm{donor}} = (35 \pm 2.5)\ M_\odot$ in our COSMIC models is compared to a single grid of MESA simulations with $M_{\mathrm{donor}} = 35M_\odot$. We also approximate all H-rich stars in COSMIC as MS stars in our MESA simulations. To determine which systems form BBHs, the HMXB population is then evolved to end of life with both COSMIC and with nearest neighbor interpolation in terms of orbital period and mass ratio of the MESA runs following Gallegos-Garcia et al. (2021). A diagram of our method is shown in Figure 1.

For each subpopulation, we label different final outcomes for Case-A HMXBs, which includes those that form BBHs. From this we calculate f_{forward}, the fraction of systems that result in each of the outcomes. We also calculate f_{backward}, the fraction of BBHs that had a Case-A HMXB progenitor and are thus candidates for BBHs with at least one high-spin BH.

2.1. *Stellar & Binary Physics*

We make use of the grids of MESA simulations from Gallegos-Garcia et al. (2021), and calculate an additional grid of simulations with $M_{\mathrm{donor}} = 45M_\odot$. Our models are initialized at a metallicity of $Z = 0.1Z_\odot$, defining $Z_\odot = 0.0142$ and $Y_\odot = 0.2703$ (Asplund et al. 2009). We also simulate one model at solar metallicity. We specify the helium fraction as $Y = Y_{\mathrm{Big\ Bang}} + (Y_\odot - Y_{\mathrm{Big\ Bang}})Z/Z_\odot$, where $Y_{\mathrm{Big\ Bang}} = 0.249$ (Ade et al. 2016). For simulations run with COSMIC, the stellar and binary physics parameters are the same as in Gallegos-Garcia et al. (2021), except now all simulations are updated to have MT prescriptions from Claeys et al. (2014).

As in Gallegos-Garcia et al. (2021), we are careful to maintain consistency among the stellar and binary physics parameters between the two codes. The COSMIC wind prescription most similar to the prescription used in our MESA simulations treats O and B stars following Vink et al. (2001), and Wolf–Rayet stars following Hamann & Koesterke (1998) reduced by factor of 10 (Yoon et al. 2010) with metallicity scaling of $(Z/Z_\odot)^{0.86}$ (Vink & de Koter 2005). For the formation of BHs, when MESA models reach core carbon depletion (central ^{12}C abundance $< 10^{-2}$), they are assumed to undergo direct core collapse to a BH with mass equal to their baryonic mass. In COSMIC, we follow the Delayed prescription of Fryer et al. (2012). We expect the small differences between the winds and supernova prescriptions for MESA and COSMIC to not significantly affect our results.

Our method for identifying high-spin HMXBs relies on Case-A MT while both stars are still on the MS. In Qin et al. (2019), this scenario was modeled using detailed MESA simulations that focused on the MT episode and binary evolution before the first BH was formed. In our study, we only model this Case-A MT stage of evolution with COSMIC, which likely results in differences between simulations performed with MESA. In a preliminary study, over a small parameter space in donor mass and orbital period, we found that in some cases, simulations ran with COSMIC tended to overestimate the number of Case-A HMXBs by roughly an factor of two compared to Figure 2 in Qin et al. (2019). We therefore treat the Case-A HMXBs populations in COSMIC as upper limits.

The evolution of Case-A MT occurs at low initial orbital periods ($\lesssim$ 25 days). At these periods, common envelope (CE) evolution is expected to be unsuccessful at removing the envelope given the energy budget formalism (van den Heuvel 1976; Webbink 1984; Ivanova 2011). As a result, at these low periods, BBH mergers can only form through stable MT (or chemically homogeneous evolution (Marchant et al. 2016; de Mink & Mandel 2016)). The mass-ratio threshold q_{crit} that sets the stability of MT for these donors (i.e., whether a system undergoes CE) therefore determines how many systems will be able to form BBHs through stable MT. If the mass ratio $q = M_{accretor}/M_{donor}$ is less than q_{crit}, the system enters unstable MT and a CE forms. A smaller q_{crit} value means fewer systems undergo CE. To explore uncertainties in this part of binary evolution, in the COSMIC models presented here, we vary the critical mass ratios by considering three different q_{crit} prescriptions following Belczynski et al. (2008), Neijssel et al. (2019), and Claeys et al. (2014). This is separate from the MT prescription, which sets the rate of mass lost from the donor star and follows Claeys et al. (2014) for all COSMIC simulations.

Case-A MT between two MS stars is the first evolutionary phase where q_{crit} becomes important in our simulations. Out of the set of q_{crit} prescriptions we consider, the model following Belczynski et al. (2008) allows more MS stars to proceed with stable MT instead of CE. For this model, all H-rich donors in binaries with mass ratios larger than $q_{crit} = 0.33$ are assumed to be stable. Neijssel et al. (2019) has the second largest q_{crit} value for MT when the donor is on MS with $q_{crit} = 0.58$. This is followed by Claeys et al. (2014), which uses $q_{crit} = 0.625$. The differences among q_{crit} are important, as they can affect the resulting population of Case-A HMXBs.

Equally as important are the q_{crit} values for Roche lobe overflow during the HMXB phase. Generally, these H-rich stars include Hertzsprung gap (HG), first giant branch, core helium burning, early asymptotic giant branch (AGB), and thermally pulsing AGB stars. For the population of Case-A HMXBs, the most evolved H-rich star in our BH–H-rich star population is a HG star. For systems containing BH–HG stars, the Claeys et al. (2014), Neijssel et al. (2019) and Belczynski et al. (2008) prescriptions use $q_{crit} = 0.21$, $q_{crit} = 0.26$ and $q_{crit} = 0.33$, respectively. For MT from a first giant branch, early AGB, and thermally pulsing AGB star onto a BH, Neijssel et al. (2019) uses the fits from Hjellming & Webbink (1987), while Claeys et al. (2014) uses $q_{crit} = 0.87$ for the same stellar types. Although these donor types are not important for progenitors of high-spin HMXBs, they can be progenitors of BBHs.

In Gallegos-Garcia et al. (2021) we found that according to detailed binary evolution calculations with MESA the dominant channel for BBHs is different compared to results from BSE-like codes using single-star evolution formulae; consequently, these rapid population-synthesis codes may be overestimating the number and rate of BBHs. By using similar methods and stellar and binary physics parameters as in Gallegos-Garcia et al. (2021), these differences should also be reflected in the results presented here. Therefore, we can asses whether our results for the contribution of Case-A HMXBs systems in the population of BBHs are robust across these two estimates for the number of BBHs.

3. RESULTS

In this section we show the outcomes of Case-A HMXBs, i.e., binaries that are assumed to be candidates for high-spin HMXBs following a phase of Case-A MT while both stars are on the MS (Section 3.1). We also quantify how many of these Case-A HMXBs form BBHs, and what fraction of the total BBHs in the population had Case-A HMXB progenitors (Section 3.2).

3.1. *Outcomes of Case-A HMXBs*

We label four different final outcomes for Case-A HMXBs for models simulated with COSMIC, and one outcome for the grids of MESA simulations. These outcomes are the following.

1. Binaries that merge during CE. These binaries are concentrated at unequal mass ratios q for all masses and model variations. We label them as failed CE.

2. Binaries that result in wide neutron star–BHs (NS-BHs) that will not merge within a Hubble time. This outcome only occurs for the least massive donor and we label them as wide NSBH.
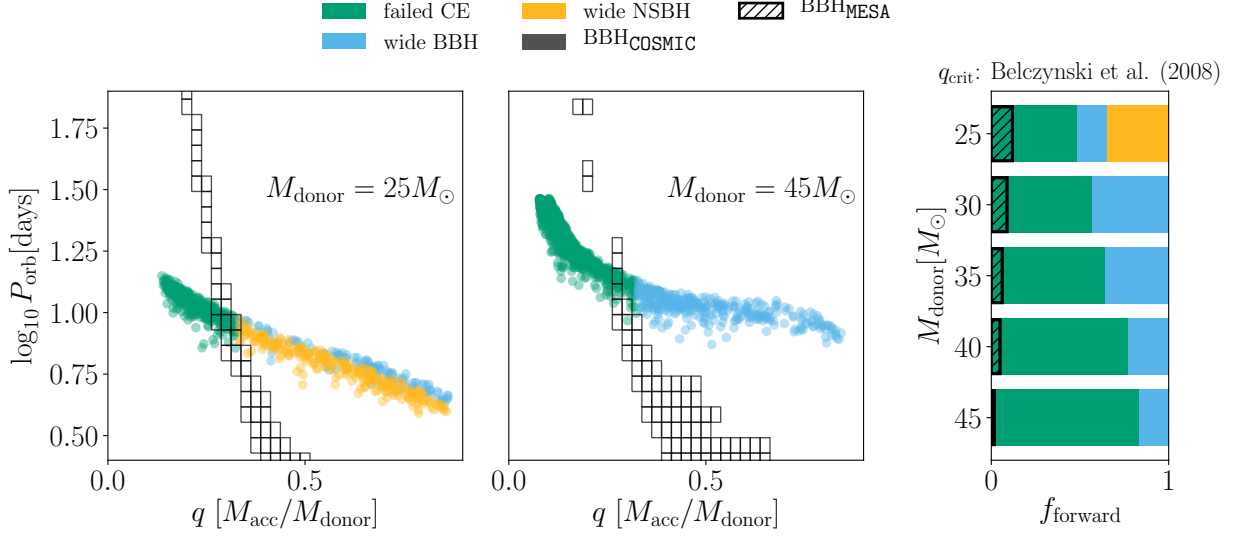
Figure 2. Summary of outcomes for model with $q_{\rm crit}$ following Belczynski et al. (2008) at $Z_\odot/10$. Points correspond to simulation outcomes for binaries ran with COSMIC. Left panel corresponds to donor masses within the range $M_{\rm donor} = (25 \pm 2.5)M_\odot$, and middle panel corresponds to $M_{\rm donor} = (45 \pm 2.5)M_\odot$. In these panels, black rectangles correspond to the parameter space where the corresponding grid of MESA simulations for that donor mass result in BBHs. The right panel shows the fractions of each outcome as a function of donor mass. The hatched black bar corresponds to the fraction of BBHs for each donor mass given the grids of simulations ran with MESA. In all three panels, binaries that merged during CE are shown in green, systems that resulted in wide NSBHs are in yellow, wide BBHs are in light blue, and BBH mergers within a Hubble time are shown in gray.

3. *Wide BBHs* that will not merge within a Hubble time. These systems make up most of the remainder of the binaries that do not merge during CE.

4. Binaries that result in BBHs that merge within a Hubble time. We label them as BBH$_{\rm COSMIC}$.

5. We label COSMIC Case-A HMXBs that result in BBHs following the nearest neighbors matching with the grids of MESA simulations as BBH$_{\rm MESA}$.

The comparison between BBH$_{\rm COSMIC}$ and BBH$_{\rm MESA}$ allows us to both asses how detailed models of binary evolution affect the final outcome of Case-A HMXBs and test the robustest of our final results.

Figure 2 shows the final outcomes following $q_{\rm crit}$ by Belczynski et al. (2008). We show systems with H-rich donor masses within the range $M_{\rm donor} = (25 \pm 2.5)M_\odot$ and $(45 \pm 2.5)M_\odot$ on the left and middle panels respectively. Each point in Figure 2 corresponds to a binary simulated with COSMIC, with the color representing the final outcome as described above. The outcomes are plotted as a function of mass ratio q and orbital period $P_{\rm orb}$ when the system became a BH–H-rich star, which is the starting state of the MESA simulations. On these same panels, the black rectangles show where our grids of BH–MS MESA models result in BBHs. In the right panel of Figure 2 we also show the fractions of the final outcomes $f_{\rm forward}$ as a function of donor mass. The

hatched boxes in this panel corresponds to BBH$_{\rm MESA}$, the fraction of BBHs assumed to form after combining our grids MESA simulations with the COSMIC Case-A HMXB population. The binaries that make up this fraction are those that fall within the black rectangles. For this model, when simulating binary evolution entirely with COSMIC we do not find any BBHs, BBH$_{\rm COSMIC} = 0$. When combining MESA with COSMIC simulations we find that only a small fraction, at most $\sim 12\%$, result in BBHs (Table 1). When considering all systems in this model, $M_{\rm donor} = (25\pm2.5)$–$(45\pm2.5)M_\odot$, only 5% of binaries result in BBHs. The differences in BBH$_{\rm COSMIC}$ and BBH$_{\rm MESA}$ for this model are because some Case-A HMXBs that undergo failed CE with COSMIC go through stable MT according to our grids of MESA simulations.

Figure 3 shows the same results as in Figure 2 but for the model using $q_{\rm crit}$ following Neijssel et al. (2019). For this model we show binaries with donor masses within the range $M_{\rm donor} = (30 \pm 2.5)M_\odot$ and $M_{\rm donor} = (45 \pm 2.5)M_\odot$ on the the left and middle panels respectively. In this model, no Case-A HMXBs form within the mass range $M_{\rm donor} = (25 \pm 2.5)M_\odot$. This is likely due to the larger $q_{\rm crit}$ threshold in the first phase of MS. This larger value intrinsically limits binaries with less massive secondary stars, which would otherwise become the donors in the HMXB phase, from proceeding with stable MT during the first MT phase. This model does, however, allow more BH–H-rich systems to proceed with
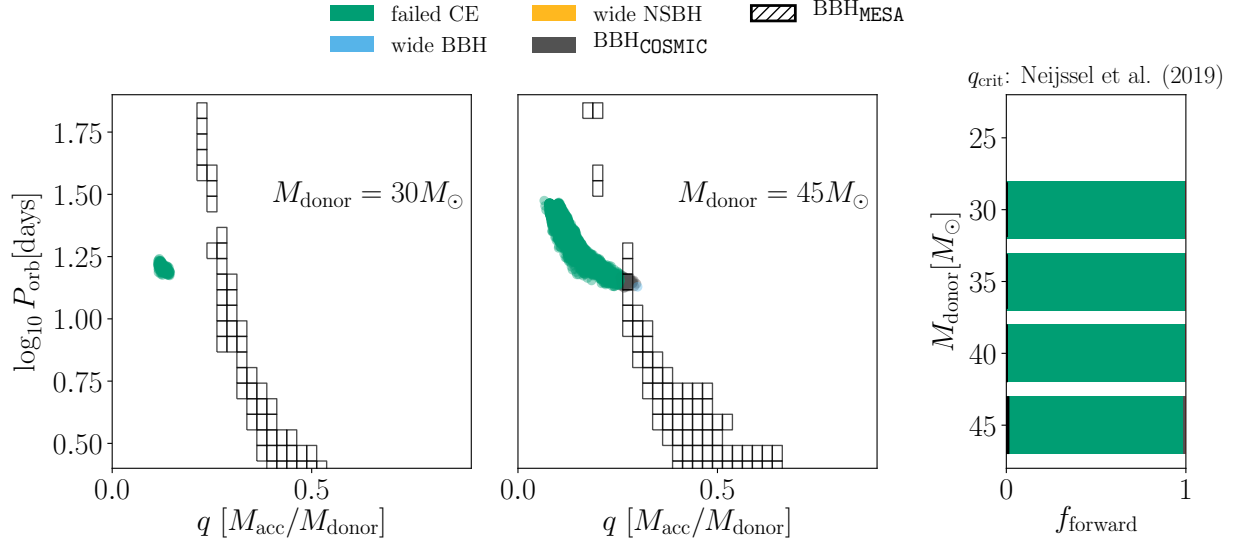
Figure 3. Same as Figure 2 but for the model using q_{crit} values following Neijssel et al. (2019). Binaries with donor masses in the range of $M_{donor} = (30 \pm 2.5)M_\odot$ are shown in the left panel and $M_{donor} = (45 \pm 2.5)M_\odot$ are shown in the middle panel. Although this model results in BBHs in the same parameter space as our grid of MESA simulations, this outcome contributes only 0.01% to the total outcome of Case-A HMXBs.

stable MT when the donor is a HG star. For donors with masses within the range $M_{donor} = (45 \pm 2.5)M_\odot$, this results in BBHs following stable MT only (gray points in middle panel). This was not the case for the model using q_{crit} following Belczynski et al. (2008). Additionally, at this donor mass, these BBHs modeled with COSMIC are consistent with the parameter space where our MESA simulations result in BBHs (the overlap of gray points and black rectangle). This is a small region in parameter space for both COSMIC and MESA with a width in mass ratio $\Delta q \sim 0.05$ and 0.0625 dex in orbital period. Compared to Figure 2, the range of mass ratios q of Case-A HMXBs is smaller, spanning $q \approx 0.1$–0.3 compared to $q \approx 0.1$–0.8. This smaller range decreases the number of BBHs over all donor masses when the COSMIC Case-A HMXB population is combined our grids of MESA simulations. This can be seen in the right-most panels of Figure 2 and Figure 3. Although the COSMIC Case-A HMXB population is different for these two models, we find similar results for the fraction of Case-A HMXBs that result in BBHs. As in the model using q_{crit} following Belczynski et al. (2008), this model does not result in a significant fraction of BBHs.

In our third model we use q_{crit} prescriptions following Claeys et al. (2014). This model results in similar BBH factions and qualitatively similar Case-A HMXB populations to the model using q_{crit} following Neijssel et al. (2019). The Case-A HMXB populations for this model have smaller mass ratio range with $q \approx 0.1$–0.25. As a result, unlike the model using q_{crit} from Neijssel et al.

(2019), we do not find an overlapping region between COSMIC BBHs from the Case-A HMXB population and BBHs simulated with MESA. For all but the most massive donor, all Case-A HMXBs result in mergers during CE.

A summary of the final outcomes for all three models is shown in Table 1. The inner four columns correspond to the different final outcomes from the COSMIC simulations. The last column corresponds to the fraction of binaries that resulted in BBHs after combining the COSMIC Case-A HMXB population with our grids of MESA simulations. These are the same values as in the right panels in Figure 2 and Figure 3.

In addition to these models, we also simulated a population of binaries at solar metallicity and found no BBHs with Case-A HMXBs progenitors with either COSMIC or MESA. This is likely due to stronger winds at solar metallicities implemented in both codes that widen the orbits and reduce the number of BBHs. We also assessed whether the fractions of Case-A HMXBs resulting in BBHs are affected by different initial binary parameter distributions. Choosing each initial ZAMS parameter of the binary independently rather than choosing them jointly as in our default Moe & Di Stefano (2017) initial distributions, we found a change of at most 1.8 in the values of BBH$_{MESA}$ and BBH$_{COSMIC}$ assuming q_{crit} follows Neijssel et al. (2019). For the model following Belczynski et al. (2008), we find a negligible change for BBH$_{MESA}$.

Table 1. Fractions of the final outcomes for Case-A HMXBs, f_{forward}. We assume these systems will form a high-spin BH in a HMXBs following a phase of Case-A MT while both stars on the MS. From left to right these columns show the fractions of binaries simulated with COSMIC that resulted in BBHs, failed CE, and wide binaries that will not merge within a Hubble time (for simplicity we have combined wide NSBH and wide BBHs systems) For models following Belczynski et al. (2008) and Neijssel et al. (2019), these fractions are illustrated in Figure 2 and Figure 3, respectively.

| Model | M_{donor} | COSMIC outcome | | | $\text{BBH}_{\texttt{MESA}}$ |
		$\text{BBH}_{\texttt{COSMIC}}$	Failed CE	Wide binaries	
Belczynski et al. (2008)	$25 M_\odot$	0	0.49	0.52	0.12
	$30 M_\odot$	0	0.57	0.43	0.09
	$35 M_\odot$	0	0.64	0.36	0.06
	$40 M_\odot$	0	0.77	0.23	0.05
	$45 M_\odot$	0	0.84	0.16	0.02
Neijssel et al. (2019)	$25 M_\odot$	–	–	–	–
	$30 M_\odot$	0	1	0	0
	$35 M_\odot$	0	1	0	0
	$40 M_\odot$	0	1	0	0
	$45 M_\odot$	0.01	0.99	0	0.01
Claeys et al. (2014)	$25 M_\odot$	–	–	–	–
	$30 M_\odot$	0	1	0	0
	$35 M_\odot$	0	1	0	0
	$40 M_\odot$	0	1	0	0
	$45 M_\odot$	0.01	0.99	0	0

3.2. *Fraction of high-spin BBHs*

Although we find that only a small fraction of Case-A HMXBs form BBHs, it is possible that this population of BBHs is large enough to contribute significantly to the full population of BBHs. In addition to determining the fates of Case-A HMXBs, we must also consider the fraction of all BBHs that had a Case-A HMXB progenitor, f_{backward}.

In Figure 4 we show the COSMIC population of all BBHs regardless of their formation path (gray contours) and all Case-A HMXBs. These populations are for BH–H-rich star systems with a donor mass $M_{\text{donor}} = (45 \pm 2.5) M_\odot$ and q_{crit} following Neijssel et al. (2019), as illustrated in the middle panel in Figure 3. Figure 4 illustrates that these two populations, BBHs and Case-A HMXBs, occur in distinct regions in the $\log P_{\text{orb}}$–q parameter space. The small overlapping region at roughly $q \sim 0.26$ and $P_{\text{orb}} \sim 20$ days corresponds to Case-A HMXBs that resulted in BBHs. It is evident that these systems only comprise a small fraction of parameter space. Systems with other donor masses have broadly similar results. Below this donor mass the overlapping region is smaller. Above this donor mass, this region tends to have similar or more overlap.

In Table 2 we show the fraction f_{backward} of BBHs that had a Case-A HMXB progenitor for all our models. We show f_{backward} for systems that we follow the full evolution using only COSMIC and for systems that use our grids of MESA simulations. Columns in Table 2 correspond to the different donor mass ranges and rows correspond to the different models. These fractions tend to be small (< 0.20) which indicates that Case-A HMXB systems and BBHs likely have little association.

Similar to our results for $\text{BBH}_{\texttt{MESA}}$ and $\text{BBH}_{\texttt{COSMIC}}$, we also test the robustness of these results when implementing independently distributed initial ZAMS binary parameters compared to a multidimensional joint distribution. With an independent distribution, our results for f_{backward} for the model following q_{crit} from Neijssel et al. (2019) change by a factor of at most 5. We find a change of a factor of at most 1.8 for simulations following q_{crit} from Belczynski et al. (2008). Small variations, on the order of $\lesssim 5$, in the number of BBHs appear to be in agreement with variations on rates of BBHs due to different initial binary parameters (de Mink & Belczynski 2015; Klencki et al. 2018).
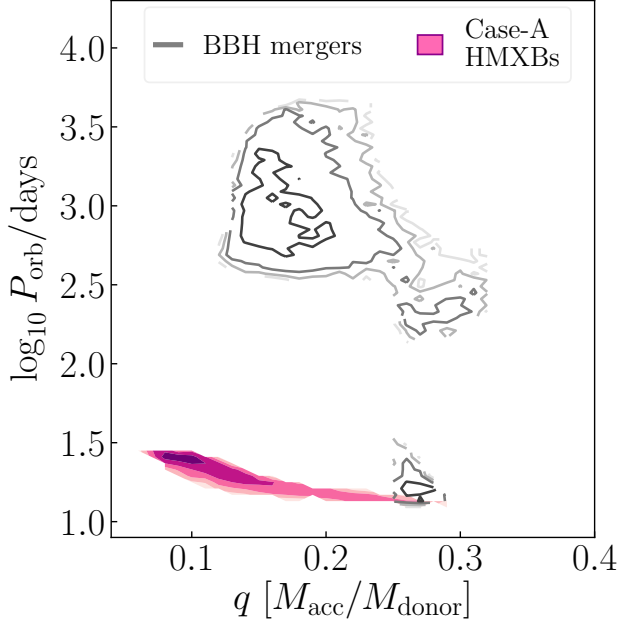
Figure 4. Contours showing the population from our `COSMIC` simulations of all BBHs regardless of their formation path (gray contours) and Case-A HMXBs (pink contours) for the model using $q_{\rm crit}$ following Neijssel et al. (2019) for systems with donor mass $M_{\rm donor} = (45 \pm 2.5) M_\odot$. These populations are shown as a function of mass ratio q and orbital period when the system became a BH–H-rich star. The overlapping region corresponds to BBHs that had Case-A HMXBs progenitors.

Table 2. The fraction $f_{\rm backward}$ of BBHs with a Case-A HMXB progenitor for the three models. From top to bottom these correspond to Belczynski et al. (2008), Neijssel et al. (2019) and Claeys et al. (2014), which we list as B+2018, N+2019, and C+2014 respectively. The top row of each model corresponds to using `COSMIC` only. The second row for each model corresponds to using our grids of BH–H-rich star simulated with `MESA`.

Model		Donor				
		$25 M_\odot$	$30 M_\odot$	$35 M_\odot$	$40 M_\odot$	$45 M_\odot$
B+2008	`COSMIC`	0	0	0	0	0
	`MESA`	0.05	0.07	0.11	0.20	0.10
N+2019	`COSMIC`	0	0	0	0	0.008
	`MESA`	0	0	0	0.001	0.039
C+2014	`COSMIC`	0	0	0	0	0.005
	`MESA`	0	0	0	0	0

4. DISCUSSION

In addition to the Case-A MT scenario adopted here (Qin et al. 2019; Valsecchi et al. 2010), several formation channels to form high-spin BHs in these binaries have been proposed. In Section 4.1 we discuss a few alternative channels for forming a high-spin BH as the first born BH in the binary and their possible contributions to the merging BBH population. In Section 4.2 we discuss a few caveats in our study and a possible avenue for improvement.

4.1. *Alternative formation scenarios for high-spin BHs in HMXBs*

One possibility for spinning up BHs in binaries is through accretion. A long-lived phase of Eddington-limited accretion can explain the high-spin BHs in low-mass X-ray binaries (Podsiadlowski et al. 2003; Fragos & McClintock 2015). In HMXBs, it is thought that the timescale for MT onto the BH is too short for Eddington-limited accretion to substantially spin up the BH (King & Kolb 1999; Fragos & McClintock 2015; Mandel & Fragos 2020). In a case study for the HMXB Cygnus X-1, using simulations ran with `MESA`, Qin et al. (2022) modeled hypercritical accretion on to a BH, where the mass accretion rate $\dot{M}$ can be a factor of $\sim 10^3$ higher than its Eddington-limited accretion rate $\dot{M}_{\rm Edd}$. They show that a near maximally spinning BH can be formed at these accretion rates under the assumptions of conservative MT and spin-up by accretion from a thin disk. This resulted in a binary that resembles Cygnus X-1 given its large uncertainties. Although Qin et al. (2022) did not model the evolution after the formation of this maximally spinning BH, it has been shown that super-Eddington accretion is inefficient at forming BBHs (van Son et al. 2020; Bavera et al. 2021; Zevin & Bavera 2022). This is because once the BH accretes significant mass and the mass ratio is reversed, conservative MT widens the orbit and prevents a BBH merger within a Hubble time. As a result, high-spin HMXBs formed via hypercritical accretion will likely not contribute significantly to the population of BBHs. However, in a recent study using `BPASS`, a population-synthesis code that models the response of the donor star to mass loss (Eldridge et al. 2017; Stanway & Eldridge 2018), Briel et al. (2022) found that super-Eddington accretion can result in binaries with significantly unequal mass ratios when the first BH is formed, enough to enable a BBH merger within a Hubble time. Whether these binaries result in a BBH merger or not, it is unclear whether hypercritical or super-Eddington accretion can effectively spin up a BH (Fragos & McClintock 2015, Section 1.2;

van Son et al. 2020, Section 5.2.3). Given these uncertainties we do not consider this scenario in this paper.

In a recent study, Shao & Li (2022) showed that a slow phase of stable Case-A MT lasting ~ 0.7 Myr from an $80 M_\odot$ MS donor onto a $30 M_\odot$ BH with an initial orbital period of 4 days can form a BBH with a component spin of ~ 0.6. This is unlike the Case-A MT studied here, which occurs between two MS stars. To achieve this, the maximum accretion rate onto the BH was relaxed to $10 \dot{M}_{\rm Edd}$ (Begelman 2002; McKinney et al. 2014). Although they show that this MT allows for more accretion onto the BH, it is not clear how common the initial conditions required for a slow phase of stable MT are in nature. Without modeling of the prior evolution that may result in these binaries, and without an informed astrophysical population, it is difficult to determine if these initial condition reflect those of HMXBs or what the contribution of these systems are to the total merging BBH population. In Gallegos-Garcia et al. (2021) we simulated MT at $10 \dot{M}_{\rm Edd}$ for grids of BH–H-rich star binaries with a maximum MS donor mass of $40 M_\odot$. We found that the BH mass can increase by at least a factor of 1.3, similar to that shown in Shao & Li (2022), but only for initial orbital periods $\lesssim 2.5$ days when the system is a BH–H-rich star binary. The contribution of BBHs from this scenario may therefore be similar to the mechanisms mentioned above that invoke accretion rates above the Eddington limit. As described for the model implementing hypercritical accretion on to a BH, we do not expect a significant contribution from these channels due to widening of the orbit and also due to possibly strict requirements on initial conditions.

High-spin BHs have also been suggested to form without invoking Roche lobe overflow accretion onto the BH. New-born BH can be spun-up during a failed or weak SN explosion (Batta et al. 2017; Schrøder et al. 2018), even if the total angular momentum of the envelope of the SN progenitor is initially zero (Antoni & Quataert 2022). Batta et al. (2017) studied this scenario using three-dimensional smooth particle hydrodynamics simulations for a BH forming in a binary. They show how a BH can be spun up by accreting SN fallback material that has been torqued by the companion during a failed SN explosion. They find that an initially non-spinning BH can reach spins of ~ 0.8, but only if the ejected material reaches distances that are comparable to the binary's separation before it is accreted. Most massive BHs are assumed to form without an explosion (Fryer et al. 2012; Ertl et al. 2020), and additionally are expected to have lost their envelope prior to core collapse (Sukhbold et al. 2016), which allows less mass to be accreted by the new-born BH. Therefore, since our donor

stars are massive, we assume this scenario does not play a large role in our populations.

It is still plausible that the spin of more massive BHs can be enhanced during a SN. Batta & Ramirez-Ruiz (2019) use an analytic formalism to calculate how the resulting mass and spin of a BH from a pre-SN He-star is affected as it accretes shells of stellar material during its direct collapse to a BH. They show that a rapidly rotating pre-SN He-star can form a BH with high spin values of > 0.8 as long as accretion feedback is inefficient. However, if accretion feedback is strong the expected spin of the BH decreases. While this scenario provides a mechanism for forming high-spin BHs in HMXBs, it depends strongly on the rotation rate of the progenitor, which we cannot extract from our simulations. As a result, we do not consider this scenario in this paper.

In addition to Case-A MT between two MS stars, Qin et al. (2019) also explored chemically homogeneous evolution (CHE; Mandel & de Mink 2016; Marchant et al. 2016; Song et al. 2016) as a way to form high-spin BHs in HMXBs. They found that while this channel can produce high-spin BHs, the orbital periods are too wide compared to observed HMXBs. While CHE can still play a role in the formation BBHs with high spin, our goal in this paper to find a scenario that can explain HMXBs with high spin. We do not consider this scenario in our analysis but leave it for future work.

These scenarios for high-spin BHs in HMXBs, including the Case-A MT scenario that forms the Case-A HMXBs studied here, all include different assumptions about stellar and binary evolution or SN physics. In the context of explaining both high-spin HMXBs and GW observations, we can straightforwardly assess the number of Case-A HMXBs in a population and model its subsequent evolution. Based on our results from Section 3, it appears to satisfy the conditions for HMXBs and BBHs. We leave more detailed analysis of the other scenarios for future work.

4.2. *Caveats and Future Work*

In this paper we investigated whether different criteria for the stability of MT, $q_{\rm crit}$, affect our results. The set of prescriptions used here are not exhaustive of those in the literature. Recent prescriptions, such as in Olejak et al. (2021), were not examined. Since the formation of Case A-HMXBs occur over a small orbital period range, and our grids of MESA simulations form BBHs over a small mass ratio range at those orbital periods, the parameter space where Case A-HMXBs can lead to BBHs is small. Therefore, we do not expect significant differences in the fractions presented here with alternative $q_{\rm crit}$ prescriptions.

For the modeling of binary evolution we performed simulations of BH–H-rich star binaries with MESA, but we only simulated MS–MS evolution with COSMIC. Similar to comparing results of BH–H-rich star outcomes in COSMIC to those from our MESA simulations, it is important to also study the prior evolution of these binaries with detailed simulations. Our results may be affected by a better implementation of MT during MS–MS evolution, and when this MT becomes unstable leading to CE.

The modeling of MS–MS evolution with COSMIC does not enable an adequate estimate of the star's core spin. As a result, we did not follow the spin evolution of the BH progenitor at any stage in our simulations. With these limitations, we have only considered the Case-A MT (while both stars on the MS) scenario for forming high-spinning HMXBs. Since it is plausible that not all Case-A HMXBs will reach high-spin values, our results should be considered conservative upper limits. Additionally, we do not consider other spin-up mechanisms and their contributions.

Most of the shortcomings associated with the need for detailed simulations can be well-addressed with population synthesis codes like POSYDON (Fragos et al. 2022), which use MESA simulations to model the full evolution of binary systems. This would also allow future studies to include higher-mass progenitors than those considered here as they simulate binary evolution with ZAMS stars up to $120 M_\odot$.

Finally, given the short orbital periods, it is plausible that Case-A HMXBs can not only form BBHs with one high-spin component, but perhaps impart non-negligible spin to the second-born BH through tides (Qin et al. 2018; Bavera et al. 2020). A more detailed study concerning the spin evolution of the second-born BH from Case-A HMXBs may help constrain the observational features expected from this small population of BBHs in GW data.

5. CONCLUSIONS

We have used grids of MESA simulations combined with the rapid population-synthesis code COSMIC to assess whether HMXBs with high-spin BHs and merging BBHs (referred to as BBHs) originate from distinct populations. To identify high-spin BHs in HMXBs, we adopted the scenario modeled in Qin et al. (2019), which shows that Case-A MT while both stars are on the MS can result in a first-born BH that is highly spinning, as long as angular momentum transport in the star is inefficient. For BHs formed outside of this Case-A MT scenario, we assume that they will have distinctively lower spin than our Case-A HMXBs.

Our main conclusions are:

1. Case-A HMXBs do not tend to form BBHs. When using only COSMIC simulations to model the full binary evolution, we find that at most 2% of Case-A HMXBs result in BBHs. When combining the COSMIC population with grids of BH–H-rich star MESA simulations, we find at most 12% form BBHs.

2. Case-A HMXBs contribute only a small fraction to the total merging BBH population. When considering all the BBHs for the range of masses investigated here, only 7% had a Case-A HMXB progenitor. When considering the individual mass ranges, the most massive H-rich donor, $M_{\mathrm{donor}} = (45 \pm 2.5) M_\odot$, had the largest fraction with at most 20% of BBHs having a Case-A HMXB progenitor.

3. The scenario of Case-A MT while both stars are on the MS allows for the formation of high-spin HMXBs while forming a minority of BBHs, such that the expected population of GW sources would contain primarily low-spin BHs.

Although a fraction of Case-A HMXBs can result in BBHs, their formation path can be significantly different from the larger BBHs population. These differences, which can lead to high-spin BHs, are important to consider when interpreting observations.

Our conclusions are in agreement with Fishbach & Kalogera (2022), who found that a subpopulation comprising of at most 30% of BBHs may have features resembling rapidly spinning HMXB-like systems, where one BH component is high-spin. This is also in agreement with Neijssel et al. (2021), who, following a case study of Cygnus X-1 and finding a 5% probability that it will result in a merging BBH within a Hubble time, infer that a small fraction of HMXBs like Cygnus X-1 may form BBHs.

In our COSMIC models we varied the mass ratio threshold for MT stability, q_{crit}, as this value determines which systems avoid CE and therefore lead to more Case-A MT systems and merging BBHs within a Hubble time. We found that different MT stability prescriptions produce significantly different populations of Case-A HMXB systems. However, the q_{crit} prescriptions produce robust conclusions and can be consistent our grids of MESA simulations. Our results also remained similar when varying metallicity in one model and the initial ZAMS binary parameters.

Incoming GW data will better resolve the spin distribution of BBHs, and as HMXB measurements improve we will have more accurate measurements of BH masses and spins in these systems. With both types of observa-

tions constraining different aspects of binary evolution, combining information from both will provide a more complete understanding of the physics of binary evolution. We can use studies like these to more accurately interpret these observed spins and to better understand the scenarios that lead to different stellar populations.

REFERENCES

Abbott, R., Abbott, T. D., Acernese, F., et al. 2021a, arXiv e-prints, arXiv:2111.03606. https://arxiv.org/abs/2111.03606

—. 2021b, arXiv e-prints, arXiv:2108.01045. https://arxiv.org/abs/2108.01045

—. 2021c, arXiv e-prints, arXiv:2111.03634. https://arxiv.org/abs/2111.03634

Abbott, R., Abbott, T. D., Abraham, S., et al. 2021d, ApJL, 913, L7, doi: 10.3847/2041-8213/abe949

—. 2021e, PhRvX, 11, 021053, doi: 10.1103/PhysRevX.11.021053

Ade, P. A. R., Aghanim, N., Arnaud, M., et al. 2016, A&A, 594, A13, doi: 10.1051/0004-6361/201525830

Ajith, P., Hannam, M., Husa, S., et al. 2011, PhRvL, 106, 241101, doi: 10.1103/PhysRevLett.106.241101

Antoni, A., & Quataert, E. 2022, MNRAS, 511, 176, doi: 10.1093/mnras/stab3776

Asplund, M., Grevesse, N., Sauval, A. J., & Scott, P. 2009, ARA&A, 47, 481, doi: 10.1146/annurev.astro.46.060407.145222

Batta, A., & Ramirez-Ruiz, E. 2019, arXiv e-prints, arXiv:1904.04835. https://arxiv.org/abs/1904.04835

Batta, A., Ramirez-Ruiz, E., & Fryer, C. 2017, ApJL, 846, L15, doi: 10.3847/2041-8213/aa8506

Bavera, S. S., Fragos, T., Qin, Y., et al. 2020, A&A, 635, A97, doi: 10.1051/0004-6361/201936204

Bavera, S. S., Fragos, T., Zevin, M., et al. 2021, A&A, doi: 10.1051/0004-6361/202039804

Begelman, M. C. 2002, ApJL, 568, L97, doi: 10.1086/340457

Belczynski, K., Bulik, T., & Bailyn, C. 2011, ApJL, 742, L2, doi: 10.1088/2041-8205/742/1/L2

Belczynski, K., Bulik, T., & Fryer, C. L. 2012, arXiv e-prints, arXiv:1208.2422. https://arxiv.org/abs/1208.2422

Belczynski, K., Kalogera, V., Rasio, F. A., et al. 2008, ApJS, 174, 223, doi: 10.1086/521026

Breivik, K., Coughlin, S., Zevin, M., et al. 2020, ApJ, 898, 71, doi: 10.3847/1538-4357/ab9d85

Briel, M. M., Stevance, H. F., & Eldridge, J. J. 2022, arXiv e-prints, arXiv:2206.13842. https://arxiv.org/abs/2206.13842

Callister, T. A., Miller, S. J., Chatziioannou, K., & Farr, W. M. 2022, arXiv e-prints, arXiv:2205.08574. https://arxiv.org/abs/2205.08574

Cantiello, M., Mankovich, C., Bildsten, L., Christensen-Dalsgaard, J., & Paxton, B. 2014, ApJ, 788, 93, doi: 10.1088/0004-637X/788/1/93

Claeys, J. S. W., Pols, O. R., Izzard, R. G., Vink, J., & Verbunt, F. W. M. 2014, A&A, 563, A83, doi: 10.1051/0004-6361/201322714

de Mink, S. E., & Belczynski, K. 2015, ApJ, 814, 58, doi: 10.1088/0004-637X/814/1/58

de Mink, S. E., & Mandel, I. 2016, MNRAS, 460, 3545, doi: 10.1093/mnras/stw1219

Eldridge, J. J., Stanway, E. R., Xiao, L., et al. 2017, PASA, 34, e058, doi: 10.1017/pasa.2017.51

Ertl, T., Woosley, S. E., Sukhbold, T., & Janka, H. T. 2020, ApJ, 890, 51, doi: 10.3847/1538-4357/ab6458

Fishbach, M., & Kalogera, V. 2022, ApJL, 929, L26,
doi: 10.3847/2041-8213/ac64a5

Fragos, T., & McClintock, J. E. 2015, ApJ, 800, 17,
doi: 10.1088/0004-637X/800/1/17

Fragos, T., Andrews, J. J., Bavera, S. S., et al. 2022, arXiv
e-prints, arXiv:2202.05892.
https://arxiv.org/abs/2202.05892

Fryer, C. L., Belczynski, K., Wiktorowicz, G., et al. 2012,
ApJ, 749, 91, doi: 10.1088/0004-637X/749/1/91

Fuller, J., Cantiello, M., Lecoanet, D., & Quataert, E. 2015,
ApJ, 810, 101, doi: 10.1088/0004-637X/810/2/101

Fuller, J., & Lu, W. 2022, MNRAS, 511, 3951,
doi: 10.1093/mnras/stac317

Fuller, J., & Ma, L. 2019, ApJL, 881, L1,
doi: 10.3847/2041-8213/ab339b

Fuller, J., Piro, A. L., & Jermyn, A. S. 2019, MNRAS, 485,
3661, doi: 10.1093/mnras/stz514

Galaudage, S., Talbot, C., Nagar, T., et al. 2021, ApJL,
921, L15, doi: 10.3847/2041-8213/ac2f3c

Gallegos-Garcia, M., Berry, C. P. L., Marchant, P., &
Kalogera, V. 2021, ApJ, 922, 110,
doi: 10.3847/1538-4357/ac2610

Hamann, W. R., & Koesterke, L. 1998, A&A, 335, 1003

Heger, A., Woosley, S. E., & Spruit, H. C. 2005, ApJ, 626,
350, doi: 10.1086/429868

Hjellming, M. S., & Webbink, R. F. 1987, ApJ, 318, 794,
doi: 10.1086/165412

Hunter, J. D. 2007, Computing in Science and Engineering,
9, 90, doi: 10.1109/MCSE.2007.55

Hurley, J. R., Tout, C. A., & Pols, O. R. 2002, MNRAS,
329, 897, doi: 10.1046/j.1365-8711.2002.05038.x

Ivanova, N. 2011, ApJ, 730, 76,
doi: 10.1088/0004-637X/730/2/76

Kimball, C., Talbot, C., Berry, C. P. L., et al. 2020, ApJ,
900, 177, doi: 10.3847/1538-4357/aba518

—. 2021, ApJL, 915, L35, doi: 10.3847/2041-8213/ac0aef

King, A. R., & Kolb, U. 1999, MNRAS, 305, 654,
doi: 10.1046/j.1365-8711.1999.02482.x

Klencki, J., Moe, M., Gladysz, W., et al. 2018, A&A, 619,
A77, doi: 10.1051/0004-6361/201833025

Liu, J., McClintock, J. E., Narayan, R., Davis, S. W., &
Orosz, J. A. 2008, ApJL, 679, L37, doi: 10.1086/588840

Mandel, I., & de Mink, S. E. 2016, MNRAS, 458, 2634,
doi: 10.1093/mnras/stw379

Mandel, I., & Fragos, T. 2020, ApJL, 895, L28,
doi: 10.3847/2041-8213/ab8e41

Marchant, P., Langer, N., Podsiadlowski, P., Tauris, T. M.,
& Moriya, T. J. 2016, A&A, 588, A50,
doi: 10.1051/0004-6361/201628133

McKinney. 2010, in Proceedings of the 9th Python in
Science Conference, ed. Stéfan van der Walt & Jarrod
Millman, 56 – 61, doi: 10.25080/Majora-92bf1922-00a

McKinney, J. C., Tchekhovskoy, A., Sadowski, A., &
Narayan, R. 2014, MNRAS, 441, 3177,
doi: 10.1093/mnras/stu762

Miller-Jones, J. C. A., Bahramian, A., Orosz, J. A., et al.
2021, Science, 371, 1046, doi: 10.1126/science.abb3363

Moe, M., & Di Stefano, R. 2017, ApJS, 230, 15,
doi: 10.3847/1538-4365/aa6fb6

Mould, M., Gerosa, D., Broekgaarden, F. S., & Steinle, N.
2022, arXiv e-prints, arXiv:2205.12329.
https://arxiv.org/abs/2205.12329

Neijssel, C. J., Vinciguerra, S., Vigna-Gómez, A., et al.
2021, ApJ, 908, 118, doi: 10.3847/1538-4357/abde4a

Neijssel, C. J., Vigna-Gómez, A., Stevenson, S., et al. 2019,
MNRAS, 490, 3740, doi: 10.1093/mnras/stz2840

Olejak, A., Belczynski, K., & Ivanova, N. 2021, A&A, 651,
A100, doi: 10.1051/0004-6361/202140520

Paxton, B., Bildsten, L., Dotter, A., et al. 2011, ApJS, 192,
3, doi: 10.1088/0067-0049/192/1/3

Paxton, B., Cantiello, M., Arras, P., et al. 2013, ApJS, 208,
4, doi: 10.1088/0067-0049/208/1/4

Paxton, B., Marchant, P., Schwab, J., et al. 2015, ApJS,
220, 15, doi: 10.1088/0067-0049/220/1/15

Paxton, B., Smolec, R., Schwab, J., et al. 2019, ApJS, 243,
10, doi: 10.3847/1538-4365/ab2241

Podsiadlowski, P., Rappaport, S., & Han, Z. 2003,
MNRAS, 341, 385, doi: 10.1046/j.1365-8711.2003.06464.x

Qin, Y., Fragos, T., Meynet, G., et al. 2018, A&A, 616,
A28, doi: 10.1051/0004-6361/201832839

Qin, Y., Marchant, P., Fragos, T., Meynet, G., & Kalogera,
V. 2019, ApJL, 870, L18, doi: 10.3847/2041-8213/aaf97b

Qin, Y., Shu, X., Yi, S., & Wang, Y.-Z. 2022, Research in
Astronomy and Astrophysics, 22, 035023,
doi: 10.1088/1674-4527/ac4ca4

Remillard, R. A., & McClintock, J. E. 2006, ARA&A, 44,
49, doi: 10.1146/annurev.astro.44.051905.092532

Reynolds, C. S. 2021, ARA&A, 59,
doi: 10.1146/annurev-astro-112420-035022

Roulet, J., Chia, H. S., Olsen, S., et al. 2021, PhRvD, 104,
083010, doi: 10.1103/PhysRevD.104.083010

Roulet, J., & Zaldarriaga, M. 2019, MNRAS, 484, 4216,
doi: 10.1093/mnras/stz226

Santamaría, L., Ohme, F., Ajith, P., et al. 2010, PhRvD,
82, 064016, doi: 10.1103/PhysRevD.82.064016

Schrøder, S. L., Batta, A., & Ramirez-Ruiz, E. 2018, ApJL,
862, L3, doi: 10.3847/2041-8213/aacf8d

Shao, Y., & Li, X.-D. 2022, ApJ, 930, 26,
doi: 10.3847/1538-4357/ac61da

Song, H. F., Meynet, G., Maeder, A., Ekström, S., & Eggenberger, P. 2016, A&A, 585, A120, doi: 10.1051/0004-6361/201526074

Spruit, H. C. 1999, A&A, 349, 189. https://arxiv.org/abs/astro-ph/9907138

Stanway, E. R., & Eldridge, J. J. 2018, MNRAS, 479, 75, doi: 10.1093/mnras/sty1353

Suijs, M. P. L., Langer, N., Poelarends, A. J., et al. 2008, A&A, 481, L87, doi: 10.1051/0004-6361:200809411

Sukhbold, T., Ertl, T., Woosley, S. E., Brown, J. M., & Janka, H. T. 2016, ApJ, 821, 38, doi: 10.3847/0004-637X/821/1/38

Valsecchi, F., Glebbeek, E., Farr, W. M., et al. 2010, Nature, 468, 77, doi: 10.1038/nature09463

van den Heuvel, E. P. J. 1976, in IAU Symposium, Vol. 73, Structure and Evolution of Close Binary Systems, ed. P. Eggleton, S. Mitton, & J. Whelan, 35

van den Heuvel, E. P. J. 2019, IAU Symposium, 346, 1, doi: 10.1017/S1743921319001315

van der Walt, S., Colbert, S. C., & Varoquaux, G. 2011, Computing in Science and Engineering, 13, 22, doi: 10.1109/MCSE.2011.37

van Son, L. A. C., De Mink, S. E., Broekgaarden, F. S., et al. 2020, ApJ, 897, 100, doi: 10.3847/1538-4357/ab9809

Vink, J. S., & de Koter, A. 2005, A&A, 442, 587, doi: 10.1051/0004-6361:20052862

Vink, J. S., de Koter, A., & Lamers, H. J. G. L. M. 2001, A&A, 369, 574, doi: 10.1051/0004-6361:20010127

Webbink, R. F. 1984, ApJ, 277, 355, doi: 10.1086/161701

Yoon, S. C., Woosley, S. E., & Langer, N. 2010, ApJ, 725, 940, doi: 10.1088/0004-637X/725/1/940

Zevin, M., & Bavera, S. S. 2022, ApJ, 933, 86, doi: 10.3847/1538-4357/ac6f5d